


# Rising synchrony controls western North American ecosystems

Bryan A. Black<sup>1</sup>  | Peter van der Sleen<sup>1</sup> | Emanuele Di Lorenzo<sup>2</sup> | Daniel Griffin<sup>3</sup> | William J. Sydeman<sup>4</sup> | Jason B. Dunham<sup>5</sup> | Ryan R. Rykaczewski<sup>6</sup> | Marisol García-Reyes<sup>4</sup> | Mohammad Safeeq<sup>7,8</sup> | Ivan Arismendi<sup>9</sup> | Steven J. Bograd<sup>10</sup>

<sup>1</sup>University of Texas Marine Science Institute, Port Aransas, TX, USA

<sup>2</sup>School of Earth & Atmospheric Sciences, Georgia Institute of Technology, Atlanta, GA, USA

<sup>3</sup>Department of Geography, Environment & Society, University of Minnesota, Minneapolis, MN, USA

<sup>4</sup>Farallon Institute for Advanced Ecosystem Research, Petaluma, CA, USA

<sup>5</sup>U.S. Geological Survey, Forest and Rangeland Ecosystem Science Center, Corvallis, OR, USA

<sup>6</sup>Department of Biological Sciences and Marine Science Program, University of South Carolina, Columbia, SC, USA

<sup>7</sup>Sierra Nevada Research Institute, University of California, Merced, CA, USA

<sup>8</sup>Pacific Southwest Research Station, USDA Forest Service, Fresno, CA, USA

<sup>9</sup>Department of Fisheries and Wildlife, Oregon State University, Corvallis, OR, USA

<sup>10</sup> Environmental Research Division, Southwest Fisheries Science Center, NOAA, Monterey, CA, USA

## Correspondence

Bryan A. Black, University of Texas Marine Science Institute, Port Aransas, TX, USA.  
Email: bryan.black@utexas.edu

## Funding information

US National Science Foundation Division of Ocean Sciences, Grant/Award Number: 1434732

## Abstract

Along the western margin of North America, the winter expression of the North Pacific High (NPH) strongly influences interannual variability in coastal upwelling, storm track position, precipitation, and river discharge. Coherence among these factors induces covariance among physical and biological processes across adjacent marine and terrestrial ecosystems. Here, we show that over the past century the degree and spatial extent of this covariance (synchrony) has substantially increased, and is coincident with rising variance in the winter NPH. Furthermore, centuries-long blue oak (*Quercus douglasii*) growth chronologies sensitive to the winter NPH provide robust evidence that modern levels of synchrony are among the highest observed in the context of the last 250 years. These trends may ultimately be linked to changing impacts of the El Niño Southern Oscillation on midlatitude ecosystems of North America. Such a rise in synchrony may destabilize ecosystems, expose populations to higher risks of extinction, and is thus a concern given the broad biological relevance of winter climate to biological systems.

## KEYWORDS

El Niño Southern Oscillation, Moran effect, North Pacific High, synchrony

## 1 | INTRODUCTION

Biological impacts of climate change have been widely documented across the world's biomes, yet such responses are almost exclusively described in terms of trends in average conditions (Parmesan & Yohe, 2003; Poloczanska et al., 2013). It is widely acknowledged, however, that global warming is also likely to increase climate

variance (Coumou & Rahmstorf, 2012; Easterling et al., 2000), the extent and consequences of which remain poorly understood. Of concern is that extreme events which often disproportionately influence biological processes and impart long-lasting effects on ecosystems, may increase in frequency (Jentsch, Kreyling, & Beierkuhnlein, 2007; Thompson, Beardall, Beringer, Grace, & Sardina, 2013). Rising climate variability may also induce synchrony in the dynamics of

spatially disjunct populations (i.e., the Moran effect (Moran, 1953)), thereby reducing the survivorship of potential emigrants available to “rescue” failing subpopulations in the event of a deleterious climate event. Such a decrease in the regional diversity of biological response to climate could potentially destabilize ecosystem processes and the services they provide to society (Harrison & Quinn, 1989; Palmqvist & Lundberg, 1998; Schindler, Armstrong, & Reed, 2015). Thus, identifying long-term trends in environmental variability or synchrony is of critical importance, especially if a given climate driver is broadly relevant to biology.

Off the coast of western North America, high winter (January–March) atmospheric pressure (i.e., the North Pacific High; NPH) is associated with more intense northwesterly, upwelling-favorable alongshore winds that lift deep, cold, nutrient-rich waters into the photic zone to stimulate production in the California Current (Huyer, 1983). At the same time, the high pressure ridge deflects Pacific storms, leading to drought on land. Thus, anomalies in winter NPH amplitude and positioning induce negative covariance between metrics of marine and terrestrial biological productivity that are sensitive to cool-season climate. For example, years of robust coastal upwelling, high seabird reproductive success, rapid rockfish growth, and lipid-rich copepod communities are associated with low precipitation and poor blue oak radial growth on land (Black et al., 2014). Although there is almost no trend in average values, centennial-length instrumental records suggest that NPH-induced winter climate variability has increased substantially over the course of the 20th century (Black et al., 2014) with concomitant effects on biological indicators (Sydeman, Santora, Thompson, Marinovic, & Di Lorenzo, 2013). Here, we utilize some of the longest spatially resolved observational records from western North America to explore how the geographic extent, magnitude, and coherence of ecosystem anomalies, including physical and biological indicators, have changed over the past century. We find that rising variance in the NPH has synchronized processes not only within but also among marine, terrestrial, and freshwater systems of western North America.

## 2 | MATERIALS AND METHODS

### 2.1 | Physical data

The winter NPH was defined as mean Jan-Mar Hadley Centre HadSLP2 sea level pressure [<http://www.metoffice.gov.uk/hadobs/hadslp2/>] for the region 25°N–35°N by 125°W–145°W, the approximate location over which the NPH is centered during the winter months (Schroder et al., 2013). Although NPH data are available prior to 1920, time series were truncated at this date due to concerns about relatively low densities of sea level pressure observations early in the 20th century. Annual water year (October 1 to September 30) discharge data (referred to as “annual discharge”) were obtained from the US Geological Survey [<https://waterdata.usgs.gov/nwis>] for relatively undisturbed watersheds in the western US states of Washington, Oregon, Idaho, California, Nevada, Arizona,

New Mexico, Utah, and Colorado (Falcone, Carlisle, Wolock, & Meador, 2010). Over half of the sites (56%) used in the variance and synchrony analysis (see below) are part of the Hydro-Climatic Data Network, a subset of US Geological Survey streamgage sites for which flow of the watercourse is natural and record length sufficiently long to analyze discharge patterns over time (Slack, Jumb, & Landweh, 1993) (Table S1). The coastal upwelling index represents the magnitude of offshore Ekman transport (Bakun, 1973; Schwing, O’farrell, Steger, & Baltz, 1996), and monthly means were obtained from the National Oceanic and Atmospheric Administration (NOAA) Pacific Fisheries Environmental Laboratory [<http://www.pfeg.noaa.gov/products/PFEL/modeled/indices/upwelling/upwelling.html>].

Monthly averaged sea level data were obtained from the University of Hawaii Sea Level Center [<http://uhslc.soest.hawaii.edu/>] for all records along the west coast of North America that exceeded at least 30 years in length. All linear trends were removed from sea level data given their possible association with tectonic processes or anthropogenic sea level rise. Monthly averaged precipitation data were obtained from two sources, the first of which was NOAA divisional data for Washington, Oregon, Idaho, California, Nevada, Arizona, New Mexico, Utah, and Colorado, available at (<https://www7.ncdc.noaa.gov/CDO/CDODivisionalSelect.jsp>). The second source was the Climate Research Unit TS3.24 gridded 0.5° precipitation data for North America (Harris, Jones, Osborn, & Lister, 2014). With the exception of river discharge, winter (January–March) means were used in all analyses.

### 2.2 | Tree-ring data

Blue oak (*Quercus douglasii*) tree-ring data were obtained through the NOAA International Tree-Ring Databank [<http://www.ncdc.noaa.gov/paleo/treering.html>]. Only growth chronologies that significantly ( $p < .01$ ) correlated with the winter NPH, extended past 2003, and had measurement time series >400 years in length were retained ( $n = 16$  time series). Measurements were standardized using negative exponential detrending in the program ARSTAN (Cook & Krusic, 2005). The Expressed Population Signal (EPS) was used to quantify how well the chronology developed from a given number of trees represents the theoretical population from which it was sampled. The “standard” chronology was retained and truncated where the Expressed Population Signal (EPS) fell below 0.85 (Wigley, Briffa, & Jones, 1984). Albeit arbitrary, an  $\text{EPS} \geq 0.85$  is often used as a threshold at which the chronology is considered sufficiently robust for climate reconstruction.

### 2.3 | Trends in variance and synchrony

The focus of this study was on those variables that related to the NPH. Thus, time series were screened for a winter NPH Pearson correlation at values of  $r < -.4$  for river discharge,  $r > .4$  for upwelling,  $r < -.5$  for sea level and NOAA divisional precipitation, and  $r < -.6$  for CRU gridded precipitation) over the interval 1948 through 2015. These thresholds accounted for the fact that some

variables were inherently more strongly correlated with NPH than others, which helped focus the geography of the analysis. Note that the findings of this study were insensitive to a single correlation threshold of 0.4 (data not shown). Prior to subsequent analysis, all time series were normalized to the common interval of 1948–2015.

To identify trends in the variance structure of time series, a running standard deviation was calculated in a 31 year window and then averaged for each variable (e.g., upwelling, sea level, river discharge, etc.). Trends in synchrony were quantified by calculating mean pairwise correlation in a running 31 year window and then fitting the resulting time series with a linear regression. Mean pairwise running correlation ( $\bar{r}$ ) was calculated within each variable (e.g., the eight upwelling time series and then the five sea level time series, etc.). Next,  $\bar{r}$  was calculated among the means of each variable type (NPH, mean river discharge, mean upwelling, mean sea level, and mean CRU precipitation) to identify trends in synchrony across marine, terrestrial, and freshwater systems. For the blue oak,  $\bar{r}$  (synchrony) was calculated for each subset of chronologies, beginning with all 16 and then repeating with the 15 longest, the 14 longest, etc., to maximize the length of the synchrony history. Results were highly consistent for 14 or more chronologies, but became less stable at lower sample depths (data not shown). This is likely due to the concentration of relatively short chronologies to the north and the resulting changes in geographic representation farther back through time.

Significance of trends in  $\bar{r}$  was evaluated by comparing observed slopes in  $\bar{r}$  to those in simulated, bootstrapped data ( $n = 10,000$  iterations). For each iteration, time series of identical number, length, and autocorrelation as the observational records were generated after which  $\bar{r}$  was calculated and fit with a linear regression. The  $\bar{r}$  regression slope from observed data was compared to the distribution slopes in the simulated data. To verify the cause of synchrony trends, each instrumental time series was regressed against winter NPH and the running correlation and regression analysis repeated on the residuals. The  $\bar{r}$  slopes were compared between the observed (unaltered) data and that from which the NPH signal had been removed.

## 3 | RESULTS

### 3.1 | Rising variance and synchrony

Running standard deviations indicate that variance has increased over the 20th century within our network of marine, freshwater, and terrestrial indicators (Figure 1a). Patterns in exceptionally long sea level records at San Francisco and San Diego closely track those in regional precipitation and the NPH (Figure 1a). Furthermore, centennial-length trends in rising variance are accompanied by rising synchrony, calculated within each variable type (rivers, upwelling, precipitation, etc.) as mean pairwise correlation ( $\bar{r}$ ) (Figure 1b). Strikingly, synchrony not only rose within these variable types but also among them (Figure 1c,d). Collectively, these findings suggest that climate-driven covariance is strengthening concurrently across marine–terrestrial–freshwater environments. Observed directional

changes in synchrony are unlikely due to chance alone, as confirmed by comparing slopes in  $\bar{r}$  to those in simulated data (see Methods; Figure S1, Table S3). When NPH signals were removed from instrumental records, trends in synchrony were no longer significant (Table S3), indicating that variability in NPH was a dominant factor driving synchrony among time series considered in this study.

### 3.2 | Enlarged NPH footprint

Coincident with rising  $\bar{r}$ , the climatological “footprint” of the winter climate pattern has expanded as evidenced by stronger correlations across the region between NPH and sea level, upwelling, precipitation, and river discharge during the latter half compared to the first half of the instrumental record (Figure 2). What was previously a signal specific to north-central California has in recent decades extended across the southwestern United States and northern Mexico. Moreover, river discharge at many sites in Oregon and Washington that were positively correlated with the NPH early in the 20th century now negatively correlate, and agree in sign, with rivers farther south in California (Figure 2). A similar landscape-level pattern of correlations occurs if the closely related ( $r = -.85$ ;  $p < .0001$ ) and consistently sampled record of sea level at San Francisco is substituted for the NPH (Figure S2). Notably, those pairs of variables that correlated the least with one another at the beginning of the record experience the greatest increase in  $\bar{r}$  over time (Figure S3). This suggests that the spread of the NPH signal across the region is likely a key driver of rising synchrony as is the intensification of this NPH signal in those areas where NPH has been historically important. Pairs of variables that are well-correlated early in the record remain as such over time (Figure S3).

### 3.3 | Historical context

The 16 blue oak tree-ring chronologies are highly sensitive to winter climate and strongly correlate with winter precipitation (Black et al., 2014; Stahle et al., 2013), the NPH, and sea level at San Francisco (Table S2). Variance has risen in these chronologies over the past century (Black et al., 2014), as has synchrony among them (Figure 3), suggesting that environmental patterns have affected biotic phenomena, increasing coherence in interannual variability of tree growth. Indeed, the uniquely long history provided by the blue oak suggests that levels of synchrony ( $\bar{r}$ ) in the 20th century have risen to among the highest levels in the multicentennial context (Figure 3). Although  $\bar{r}$  varied considerably over the past 250 years, and in tandem with levels of variance, confidence intervals around maximum  $\bar{r}$  values (peaking in the 31 year window of 1972–2002) at least marginally exceed those of all other decades in the proxy record (Figure 3).

### 3.4 | Origins of rising synchrony

The century-length rise in variance and synchrony within and among western North American ecosystems may have linkages to the

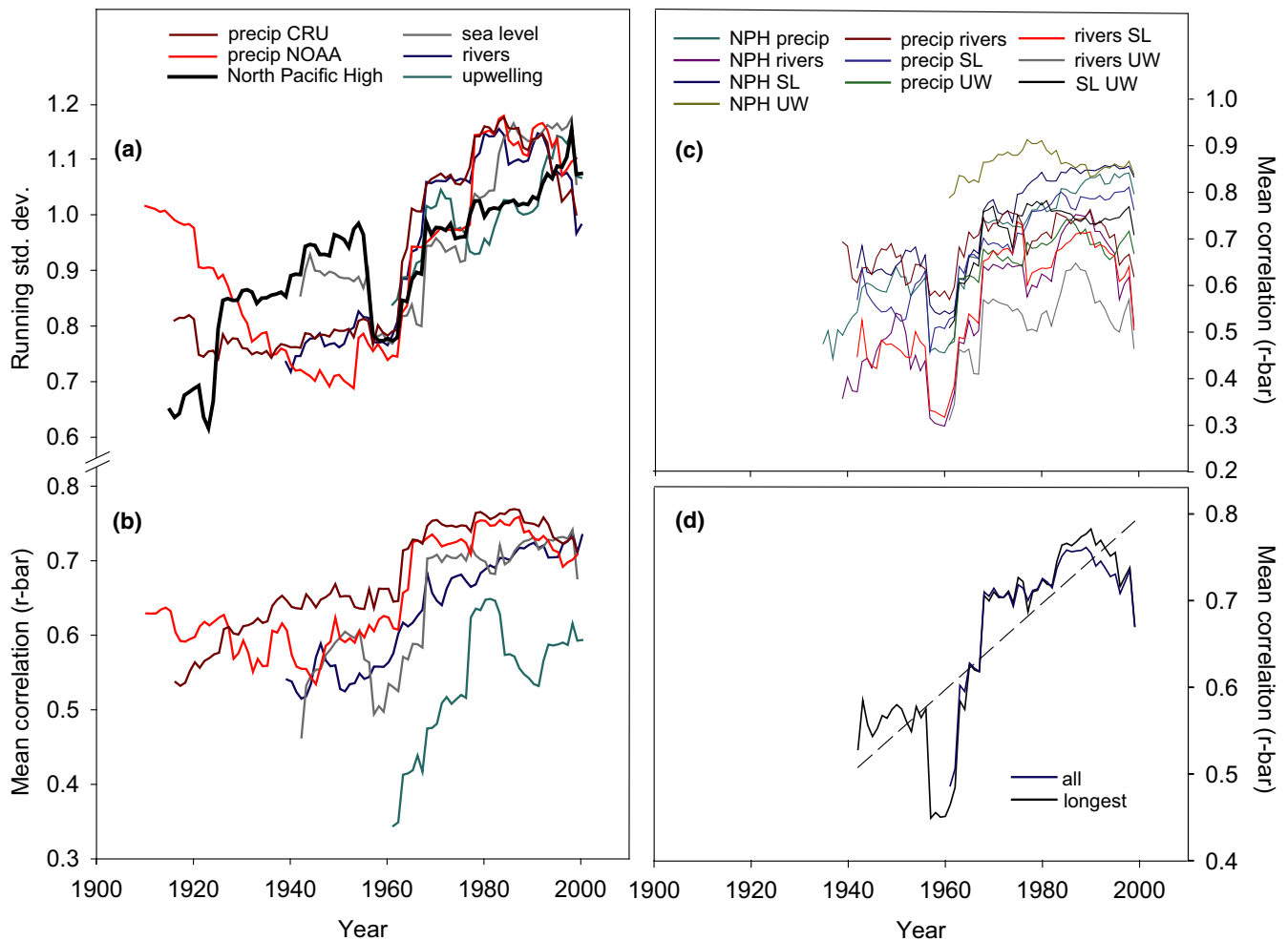


**FIGURE 1** Trends in variance and synchrony for winter climate indicators in western North America. (a) Running std dev (31 year window) for the North Pacific High, annual river discharge ( $n = 7$ ), winter sea level ( $n = 5$ ), winter upwelling ( $n = 8$ ), winter precipitation across NOAA climate divisions ( $n = 13$ ) and winter precipitation across CRU gridded data ( $n = 76$ ). (b) Mean running pairwise correlations (31 year window) within time series of annual river discharge, winter sea level, winter upwelling, winter NOAA precipitation, and winter CRU gridded precipitation. (c) Mean running pairwise correlations (31 year window) between all possible combinations of the North Pacific High (NPH), sea level averaged across five sites (SL), annual river discharge averaged across seven sites (rivers), upwelling averaged across eight sites (UW), and CRU precipitation averaged across 76 grid cells (precip). (d) Mean running pairwise correlation among these five variables (all) and a subset of the longest four variables (rivers, sea level, NPH, and CRU precipitation). Dotted line is linear trend for the "longest" subset; slope = 0.005;  $p = .04$

tropical Pacific. The winter NPH has in recent decades become much more strongly related to low-latitude atmospheric pressure fields in the vicinity of the western Pacific warm pool (Figure 4). Correlations between these regions are negligible over the 1920 through 1966 interval, intensifying to highly significant ( $p < .001$ ) levels over the more recent 1967 through 2013 interval (Figure 4). This suggests that covariance between the NPH and the tropical Pacific has substantially increased over the past hundred years. To better explore the timing and nature of these changing relationships, mean Jan-Mar Hadley Centre HadSLP2 sea level pressure was extracted from the region of the tropical western Pacific over which correlation with the NPH has increased ( $15^{\circ}\text{S}$ – $20^{\circ}\text{N}$  by  $110^{\circ}\text{E}$ – $145^{\circ}\text{E}$ ). A running (31 years) correlation between sea level pressure in the tropical Pacific and the NPH indicates a sharp increase in coupling beginning in the mid-1960s (Figure S4). However, this strengthening relationship

occurs as soon as the 31 year running window of correlation envelops the extreme El Niño event of 1983. Given their leverage on correlation coefficients, subsequent El Niño events in 1992 and 1998 help to maintain these strong relationships through present.

## 4 | DISCUSSION

### 4.1 | Evidence in biological indicators

Rising variance in the amplitude of the NPH in winter has induced a pervasive signal of rising variance and synchrony among marine, terrestrial, and freshwater ecosystems of western North America. Biological impacts consistent with such trends have been previously documented in terrestrial environments of California. Near San Francisco, extreme variability in interannual precipitation-induced

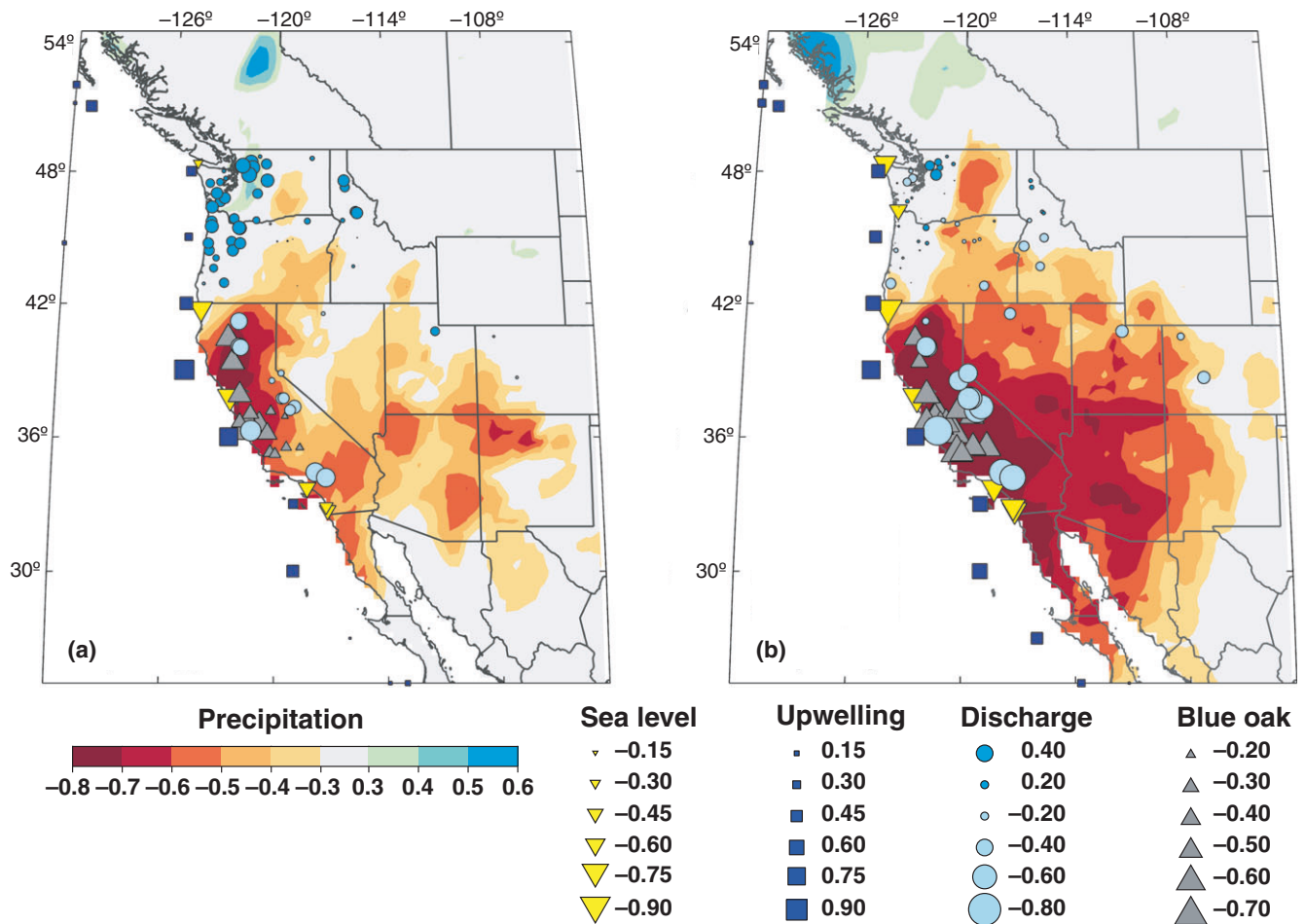


**FIGURE 2** Correlation between winter North Pacific High and winter climate indicators during the first half of the record and the second half of the record. (a) First half of the record: CRU gridded winter precipitation (1920–1967), annual river discharge (1940–1977), winter upwelling (1946–1980), winter sea level (1935–1974), and blue oak tree-ring chronologies (1920–1961). (b) Second half of the record: CRU gridded winter precipitation (1968–2014), annual river discharge (1978–2015), winter upwelling (1981–2015), winter sea level (1975–2014), and blue oak tree-ring chronologies (1962–2003)

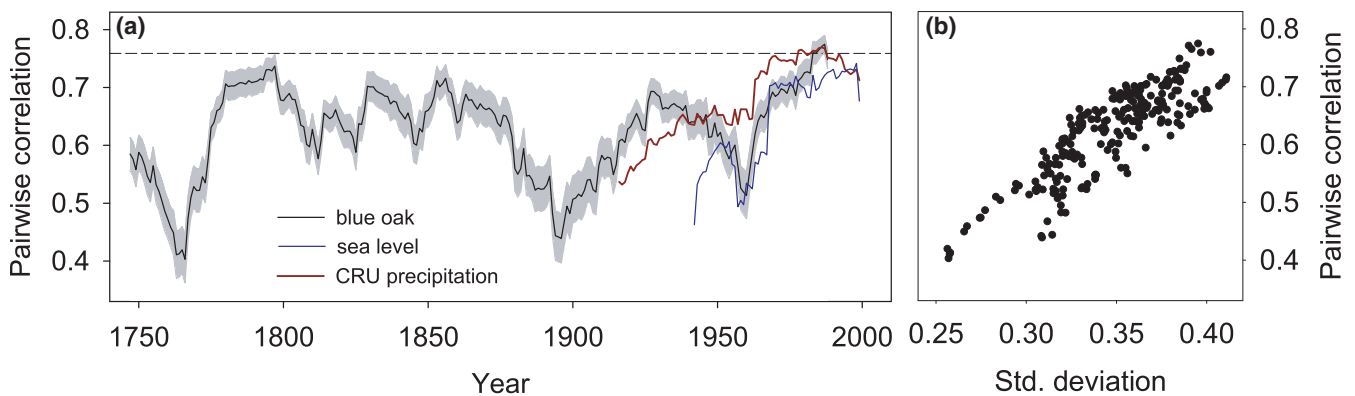


**FIGURE 3** A multicentennial history of synchrony. (a) Mean running pairwise correlations ( $\bar{r}$ ) for 16 blue oak chronologies as well as instrumental records of winter precipitation and sea level. Dotted horizontal line is the lower confidence interval for 1987, the year with the maximal  $\bar{r}$  value (corresponding to an  $\bar{r}$  window of 1972 through 2002). (b) Relationship between average running standard deviation and running  $\bar{r}$  for blue oak

temporal mismatches between larval development and the availability of host plants, collapsing two populations of checkerspot butterfly (*Euphydryas editha bayensis*) (McLaughlin, Hellmann, Boggs, &

Ehrlich, 2002). Along a 700 km latitudinal gradient from San Diego to San Francisco, *Artemisia californica* shrubs from sites in which interannual precipitation regimes are highly variable have greater

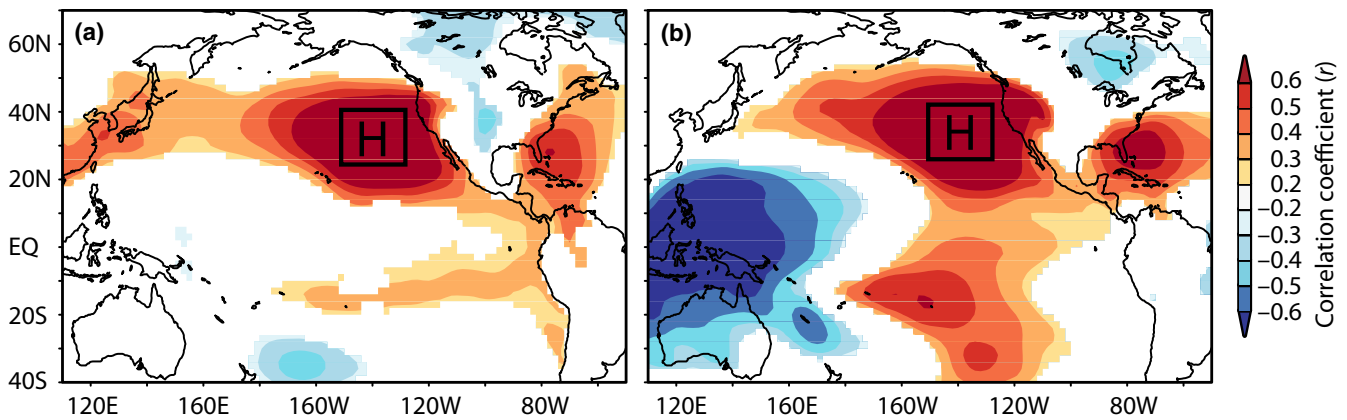


**FIGURE 4** Correlation between the winter North Pacific High (square with “H”) and winter gridded sea level pressure (20th Century Reanalysis). (a) Over the interval of 1920–1966 and (b) over the interval of 1967–2013

capacity to exploit favorable moisture conditions compared to individuals from sites in which precipitation regimes are relatively stable (Pratt & Mooney, 2013). However, over the past several decades, variability in interannual precipitation has increased, and to the greatest extent at historically stable sites where plants are less well adapted to accommodate such change (Pratt & Mooney, 2013).

With respect to the marine environment, variance in the (1) reproductive success (offspring raised per pair) of a seabird, the Cassin’s auklet (*Ptychoramphus aleuticus*) at the Farallon Islands, California, and (2) the abundance of Sacramento River fall run Chinook Salmon (*Oncorhynchus tshawytscha*) have increased (Sydeman et al., 2013), as have the variance and synchrony in survival rates of Coho (*O. kisutch*) and Chinook Salmon from Alaska through California (Kilduff, Di Lorenzo, Botsford, & Teo, 2015). Rising variance in these marine populations has been attributed to rising variance in the North Pacific Gyre Oscillation (NPGO), a mode of climate variation that correlates to patterns of nutrients, salinity, and plankton dynamics in the northeastern Pacific (Di Lorenzo et al., 2008; Sydeman et al., 2013). In turn, the variance increase in the NPGO has been linked to stronger expressions of Central Pacific El Niños (Kilduff et al., 2015), which energizes the low-frequency variability in NPGO (Di Lorenzo et al., 2010). The forcing pattern of the NPGO is an atmospheric pressure dipole with a climatological low centered on Kodiak, Alaska, and a climatological high that overlaps considerably with the winter NPH (Di Lorenzo et al., 2008). Thus, rising variance in the NPGO and NPH are likely related, although the NPH is much more strongly coupled with the geophysical indicators in this study, as well as a wide range of biological indices (Black et al., 2011; Garcia-Reyes et al., 2013; Schroder et al., 2013; Thompson et al., 2012). Our ability to detect trends in variance or synchrony in observational biological records is, however, hindered by the lack of records that span multiple decades.

## 4.2 | Origins of rising synchrony

Strengthening correlations between the winter NPH and atmospheric pressure in the western Pacific warm pool suggest that rising

synchrony and variance may be linked to changes in tropical climate and/or teleconnections to western North America. The NPH is closely coupled with a region of climatological low pressure north of Australia (Hartmann, 2015; Schwing, Murphree, & Green, 2002; Seager et al., 2015), the same area for which correlations between SLP and winter NPH have increased in recent decades (Figure 4). Both the NPH and western tropical Pacific are centers of action for North Pacific Hadley/Walker atmospheric circulation, which are heavily influenced by ENSO (Di Lorenzo et al., 2010; Furtado, Di Lorenzo, Anderson, & Schneider, 2012; Schwing et al., 2002), the variability of which has been increasing over the past hundred years to unusually or unprecedentedly high levels in the context of the past several centuries (Cai et al., 2015; Cobb, Charles, Cheng, & Edwards, 2003; Li et al., 2011; Liu et al., 2017). Thus, greater amplitude in ENSO is likely to be associated with rising variability in the winter NPH and synchrony among associated physical and biological populations in western North America. Indeed, rising variance in the tropics has been associated with a rapid succession of recent climate extremes in western North America including record-breaking El Niño events in 1982–1983, 1997–1998, and 2015–2016, and the unusually persistent 2014–2015 North Pacific Ocean heat wave known as “The Blob,” which was linked to the recent exceptional California drought (Bond, Cronin, Freeland, & Mantua, 2015; Di Lorenzo & Mantua, 2016; Griffin & Anchukaitis, 2014; Wang, Hippias, Gillies, & Yoon, 2014; Williams et al., 2015). The apparent step-change in connectivity between the NPH and sea level pressure in the western tropical Pacific appears to coincide with this series of extreme events beginning with the 1983 El Niño. Other possible mechanisms include changes in ENSO phenology or expression (Ashok & Yamagata, 2009; Zhou, Xie, Zheng, Liu, & Wang, 2014) as well as interactions with other broad-scale climate phenomena such as the Pacific Meridional Modes (Liguori & Di Lorenzo, 2018), Pacific decadal variability (Mantua & Hare, 2002), or North Pacific Gyre Oscillation (Di Lorenzo et al., 2008), among others. Ultimately, how these factors interact to influence apparent changes in the connectivity between the NPH and the tropics is unknown and worthy of study. However, the balance of evidence suggests that part of the rise in NPH

variability and related patterns of synchrony have origins in the tropics, and that the intensity of these relationships has changed over the past century.

### 4.3 | Historical context

Blue oak tree-ring chronologies confirm that the level of variance (Black et al., 2014), and especially synchrony, have risen over the past hundred years to levels that are among the highest of the 250 year reconstruction. A conspicuous feature of this longer term history, however, is the occurrence of three low-synchrony events. The most recent of these occurs in the late 1950s and 1960s and is associated with a period of relatively low variability between the large 1941 and 1983 El Niño events. Comparisons with North Pacific climate variability is complicated by poor agreement among existing reconstructions (Kipfmüller, Larson, & St George, 2012). However, the relatively asynchronous period of the 1760s in the blue oak record coincides with a period of quiescence in several ENSO reconstructions that span marine and terrestrial archives across both hemispheres and provide at least some corroborating evidence that this was a time of low tropical variability (Braganza, Gergis, Power, Risbey, & Fowler, 2009; Wilson et al., 2010). Yet the record with the greatest similarity appears to be a reconstruction of the North Atlantic Jet (NAJ) positioning derived from European tree-ring chronologies (Trouet, Babst, & Meko, 2018). All three periods of low synchrony in the blue oak record correspond to periods of low interannual NAJ variability. Further mirroring patterns in blue oak synchrony, NAJ variability is conspicuously elevated during the 1790s and also sharply increases late in the record, beginning around 1960 (Trouet et al., 2018). This suggests that general patterns of midlatitude variability may be coherent across broad spatial domains.

### 4.4 | Broader implications

The effects of climate variability on biological synchrony are widely documented. For example, growth synchrony is a central principle of modern dendrochronology that not only enables the exact dating of growth-increment time series, but also illustrates the pervasive influence of climate among individuals, habitats, and species from high-elevation forests to marine fish, corals, and bivalves (Black et al., 2016; Douglass, 1941; Fritts, 1976). Beyond growth rate, climate variability has also been linked to synchrony among population sizes with examples from insects (Allstadt, Liebhold, Johnson, Davis, & Haynes, 2015; Jepsen, Hagen, Karlsen, & Ims, 2009; Mclaughlin et al., 2002; Ojanen, Nieminen, Meyke, Poyry, & Hanski, 2013; Sheppard, Bell, Harrington, & Reuman, 2016) to vertebrates (Hansen et al., 2013; Post & Forchhammer, 2002). The synchronizing effects of climate on biology are particularly apparent following climate regime shifts, such as occurred in the North Pacific in 1977 or on an even broader global scale in the 1980s, with the potential to profoundly reorganize ecosystem structure and functioning across a range of trophic levels and spatial scales (Anderson & Piatt, 1999;

Defriez, Sheppard, Reid, & Reuman, 2016; Mantua & Hare, 2002; Reid et al., 2016).

Less common are studies that document directional trends in biological synchrony. Beyond those examples specific to this study region (Kilduff et al., 2015; Mclaughlin et al., 2002), the spatial synchrony in North American wintering bird species has increased as a consequence of rising synchrony in maximum air temperatures (Koenig & Liebhold, 2016). In Eurasia, tree-ring records indicate that forests in central Siberia have become more synchronous with those in Spain via the effects of long-term warming on growing-season length in the north and drought intensity in the south (Shestakova et al., 2016). Thus, over these broad scales, physical and biological synchrony have been enhanced by rising temperatures. Furthermore, rising temperatures have also enhanced the synchrony of snowpack as well as the occurrence of wildland fire across western North America (Kitzberger, Brown, Heyerdahl, Swetnam, & Veblen, 2007; Pederson, Betancourt, & Mccabe, 2013). As for the winter climate pattern described in the present study, there is no evidence that regional temperature is a factor in synchrony trends. Instead, synchrony trends appear to be driven by variability in the North Pacific High and its effects on precipitation and meridional winds. This is consistent with Ganguli and Ganguly (2016) who found that drought, as defined only by precipitation and not temperature, had over the past century increased in spatial coverage across the southwestern region of the United States.

Ultimately, the bottom-up forcing by the NPH illustrates that rising synchrony can be far-reaching and pervasive, simultaneously impacting marine, terrestrial, and freshwater systems. Thus, not only is this an issue within but also among ecosystems, and species that utilize more than one of these habitats to complete their life cycle may be particularly vulnerable. One notable example is Pacific salmon, for which increasing temporal and spatial synchrony may lead to decreased population production and viability (Schindler et al., 2010, 2015). Given the limited length of observational biological records and even instrumental records, high-resolution proxies will be key to establishing preindustrial, baseline ranges of synchrony as well as assessing the extent to which resilience, the stability of ecosystem processes, and diversity of biological responses to climate are reduced. Considering their possibly widespread prevalence and biological relevance, such trends in variance and synchrony should be more broadly quantified and prominently addressed in the mitigation and management of climate change impacts.

### ACKNOWLEDGEMENTS

This work was funded by the US National Science Foundation Division of Ocean Sciences award 1434732. We are also grateful to David Stahle and others who contributed to the International Tree-Ring Databank. Any use of trade, firm, or product names is for descriptive purposes only and does not imply endorsement by the US Government.

## CONFLICT OF INTEREST

The authors declare no conflict of interest, financial or otherwise.

## ORCID

Bryan A. Black  <http://orcid.org/0000-0001-6851-257X>

## REFERENCES

- Allstadt, A. J., Liebhold, A. M., Johnson, D. M., Davis, R. E., & Haynes, K. J. (2015). Temporal variation in the synchrony of weather and its consequences for spatiotemporal population dynamics. *Ecology*, *96*, 2935–2946. <https://doi.org/10.1890/14-1497.1>
- Anderson, P. J., & Piatt, J. F. (1999). Community reorganization in the Gulf of Alaska following ocean climate regime shift. *Marine Ecology Progress Series*, *189*, 117–123. <https://doi.org/10.3354/meps189117>
- Ashok, K., & Yamagata, T. (2009). The El Niño with a difference. *Nature*, *461*, 481–484. <https://doi.org/10.1038/461481a>
- Bakun, A. (1973). Coastal upwelling indices, west coast of North America, 1946–71. *Special Scientific Report, Fisheries #671*, U.S. National Oceanic and Atmospheric Administration, Seattle, WA, 103 pp.
- Black, B. A., Griffin, D., Van Der Sleen, P., Wanamaker, A. D., Speer, J. H., Frank, D. C., ... Griffin, S. (2016). The value of crossdating to retain high-frequency variability, climate signals, and extreme events in environmental proxies. *Global Change Biology*, *22*, 2582–2595. <https://doi.org/10.1111/gcb.13256>
- Black, B. A., Schroeder, I. D., Sydeman, W. J., Bograd, S. J., Wells, B. K., & Schwing, F. B. (2011). Winter and summer upwelling modes and their biological importance in the California Current Ecosystem. *Global Change Biology*, *17*, 2536–2545. <https://doi.org/10.1111/j.1365-2486.2011.02422.x>
- Black, B. A., Sydeman, W. J., Frank, D. C., Griffin, D., Stahle, D. W., García-Reyes, M., ... Peterson, W. T. (2014). Six centuries of variability and extremes in a coupled marine-terrestrial ecosystem. *Science*, *345*, 1498–1502. <https://doi.org/10.1126/science.1253209>
- Bond, N. A., Cronin, M. F., Freeland, H., & Mantua, N. (2015). Causes and impacts of the 2014 warm anomaly in the NE Pacific. *Geophysical Research Letters*, *42*, 3414–3420. <https://doi.org/10.1002/2015GL063306>
- Braganza, K., Gergis, J. L., Power, S. B., Risbey, J. S., & Fowler, A. M. (2009). A multiproxy index of the El Niño-Southern Oscillation, AD 1525–1982. *Journal of Geophysical Research-Atmospheres*, *114*, D05106. <https://doi.org/10.1029/2008JD010896>
- Cai, W., Santoso, A., Wang, G. J., Yeh, S. W., An, S. I., Cobb, K. M., ... Lengaigne, M. (2015). ENSO and greenhouse warming. *Nature Climate Change*, *5*, 849–859. <https://doi.org/10.1038/nclimate2743>
- Cobb, K. M., Charles, C. D., Cheng, H., & Edwards, R. L. (2003). El Niño/Southern Oscillation and tropical Pacific climate during the last millennium. *Nature*, *424*, 271–276. <https://doi.org/10.1038/nature01779>
- Cook, E. R., & Krusic, P. J. (2005). *ARSTAN v. 41d: A tree-ring standardization program based on detrending and autoregressive time series modeling, with interactive graphics*. Palisades, NY: Tree-Ring Laboratory, Lamont-Doherty Earth Observatory of Columbia University.
- Coumou, D., & Rahmstorf, S. (2012). A decade of weather extremes. *Nature Climate Change*, *2*, 491–496.
- Defriez, E. J., Sheppard, L. W., Reid, P. C., & Reuman, D. C. (2016). Climate change-related regime shifts have altered spatial synchrony of plankton dynamics in the North Sea. *Global Change Biology*, *22*, 2069–2080. <https://doi.org/10.1111/gcb.13229>
- Di Lorenzo, E., Cobb, K. M., Furtado, J. C., Schneider, N., Anderson, B. T., Bracco, A., ... Vimont, D. J. (2010). Central Pacific El Niño and decadal climate change in the North Pacific Ocean. *Nature Geoscience*, *3*, 762–765. <https://doi.org/10.1038/ngeo984>
- Di Lorenzo, E., & Mantua, N. (2016). Multi-year persistence of the 2014/15 North Pacific Marine Heatwave. *Nature Climate Change*, *6*, 1042–1047. <https://doi.org/10.1038/nclimate3082>
- Di Lorenzo, E., Schneider, N., Cobb, K. M., Franks, P. J. S., Chhak, K., Miller, A. J., ... Powell, T. M. (2008). North Pacific Gyre Oscillation links ocean climate and ecosystem change. *Geophysical Research Letters*, *35*, L08607. <https://doi.org/10.1029/2007GL032838>
- Douglas, A. E. (1941). Crossdating in dendrochronology. *Journal of Forestry*, *39*, 825–831.
- Easterling, D. R., Meehl, G. A., Parmesan, C., Changnon, S. A., Karl, T. R., & Mearns, L. O. (2000). Climate extremes: Observations, modeling, and impacts. *Science*, *289*, 2068–2074. <https://doi.org/10.1126/science.289.5487.2068>
- Falcone, J. A., Carlisle, D. M., Wolock, D. M., & Meador, M. R. (2010). GAGES: A stream gage database for evaluating natural and altered flow conditions in the conterminous United States. *Ecology*, *91*, 621. <https://doi.org/10.1890/09-0889.1>
- Fritts, H. C. (1976). *Tree rings and climate*. New York, NY: Academic Press.
- Furtado, J. C., Di Lorenzo, E., Anderson, B. T., & Schneider, N. (2012). Linkages between the North Pacific Oscillation and central tropical Pacific SSTs at low frequencies. *Climate Dynamics*, *39*, 2833–2846. <https://doi.org/10.1007/s00382-011-1245-4>
- Ganguli, P., & Ganguly, A. R. (2016). Space-time trends in U.S. meteorological droughts. *Journal of Hydrology: Regional Studies*, *8*, 235–259.
- García-Reyes, M., Sydeman, W. J., Black, B. A., Rykaczewski, R. R., Schoeman, D. S., Thompson, S. A., & Bograd, S. J. (2013). Relative influence of oceanic and terrestrial pressure systems in driving upwelling-favorable winds. *Geophysical Research Letters*, *40*, 5311–5315. <https://doi.org/10.1002/2013GL057729>
- Griffin, D., & Anchukaitis, K. J. (2014). How unusual is the 2012–2014 California drought? *Geophysical Research Letters*, *41*, 9017–9023. <https://doi.org/10.1002/2014GL062433>
- Hansen, B. B., Grøtan, V., Aanes, R., Sæther, B. E., Stien, A., Fuglei, E., ... Pedersen, Å. Ø. (2013). Climate events synchronize the dynamics of a resident vertebrate community in the high arctic. *Science*, *339*, 313–315. <https://doi.org/10.1126/science.1226766>
- Harris, I., Jones, P. D., Osborn, T. J., & Lister, D. H. (2014). Updated high-resolution grids of monthly climatic observations - the CRU TS3.10 Dataset. *International Journal of Climatology*, *34*, 623–642. <https://doi.org/10.1002/joc.3711>
- Harrison, S., & Quinn, J. F. (1989). Correlated environments and the persistence of metapopulations. *Oikos*, *56*, 293–298. <https://doi.org/10.2307/3565613>
- Hartmann, D. L. (2015). Pacific sea surface temperature and the winter of 2014. *Geophysical Research Letters*, *42*, 1894–1902. <https://doi.org/10.1002/2015GL063083>
- Huyer, A. (1983). Coastal upwelling in the California Current System. *Progress in Oceanography*, *12*, 259–284. [https://doi.org/10.1016/0079-6611\(83\)90010-1](https://doi.org/10.1016/0079-6611(83)90010-1)
- Jentsch, A., Kreyling, J., & Beierkuhnlein, C. (2007). A new generation of climate-change experiments: Events, not trends. *Frontiers in Ecology and the Environment*, *5*, 365–374. [https://doi.org/10.1890/1540-9295\(2007\)5\[365:ANGOCE\]2.0.CO;2](https://doi.org/10.1890/1540-9295(2007)5[365:ANGOCE]2.0.CO;2)
- Jepsen, J. U., Hagen, S. B., Karlsen, S. R., & Ims, R. A. (2009). Phase-dependent outbreak dynamics of geometrid moth linked to host plant phenology. *Proceedings of the Royal Society B-Biological Sciences*, *276*, 4119–4128. <https://doi.org/10.1098/rspb.2009.1148>
- Kilduff, D. P., Di Lorenzo, E., Botsford, L. W., & Teo, S. L. H. (2015). Changing central Pacific El Niños reduce stability of North American salmon survival rates. *Proceedings of the National Academy of Sciences of the United States of America*, *112*, 10962–10966. <https://doi.org/10.1073/pnas.1503190112>



- Kipfmüller, K. F., Larson, E. R., & St George, S. (2012). Does proxy uncertainty affect the relations inferred between the Pacific Decadal Oscillation and wildfire activity in the western United States? *Geophysical Research Letters*, *39*, L04703. <https://doi.org/10.1029/2011GL050645>
- Kitzberger, T., Brown, P. M., Heyerdahl, E. K., Swetnam, T. W., & Veblen, T. T. (2007). Contingent Pacific-Atlantic Ocean influence on multicentury wildfire synchrony over western North America. *Proceedings of the National Academy of Sciences of the United States of America*, *104*, 543–548. <https://doi.org/10.1073/pnas.0606078104>
- Koenig, W. D., & Liebhold, A. M. (2016). Temporally increasing spatial synchrony of North American temperature and bird populations. *Nature Climate Change*, *6*, 614–617. <https://doi.org/10.1038/nclimate2933>
- Li, J., Xie, S. P., Cook, E. R., Huang, G., D'Arrigo, R., Liu, F., ... Zheng, X. T. (2011). Interdecadal modulation of El Niño amplitude during the past millennium. *Nature Climate Change*, *1*, 114–118. <https://doi.org/10.1038/nclimate1086>
- Liguori, G., & Di Lorenzo, E. (2018). Meridional modes and increasing Pacific decadal variability under greenhouse forcing. *Geophysical Research Letters*, *45*, 983–991. <https://doi.org/10.1002/2017GL076548>
- Liu, Y., Cobb, K. M., Song, H., Li, Q., Li, C. Y., Nakatsuka, T., ... Leavitt, S. W. (2017). Recent enhancement of central Pacific El Niño variability relative to last eight centuries. *Nature Communications*, *8*, 15386. <https://doi.org/10.1038/ncomms15386>
- Mantua, N. J., & Hare, S. R. (2002). The Pacific decadal oscillation. *Journal of Oceanography*, *58*, 35–44. <https://doi.org/10.1023/A:1015820616384>
- Mclaughlin, J. F., Hellmann, J. J., Boggs, C. L., & Ehrlich, P. R. (2002). Climate change hastens population extinctions. *Proceedings of the National Academy of Sciences of the United States of America*, *99*, 6070–6074. <https://doi.org/10.1073/pnas.052131199>
- Moran, P. P. (1953). The statistical analysis of the Canadian Lynx cycle. 2. Synchronization and meteorology. *Australian Journal of Zoology*, *1*, 291–298. <https://doi.org/10.1071/ZO9530291>
- Ojanen, S. P., Nieminen, M., Meyke, E., Poyry, J., & Hanski, I. (2013). Long-term metapopulation study of the Glanville fritillary butterfly (*Melitaea cinxia*): Survey methods, data management, and long-term population trends. *Ecology and Evolution*, *3*, 3713–3737. <https://doi.org/10.1002/ece3.733>
- Palmqvist, E., & Lundberg, P. (1998). Population extinctions in correlated environments. *Oikos*, *83*, 359–367. <https://doi.org/10.2307/3546850>
- Parnesan, C., & Yohe, G. (2003). A globally coherent fingerprint of climate change impacts across natural systems. *Nature*, *421*, 37–42. <https://doi.org/10.1038/nature01286>
- Pederson, G. T., Betancourt, J. L., & McCabe, G. J. (2013). Regional patterns and proximal causes of the recent snowpack decline in the Rocky Mountains, US. *Geophysical Research Letters*, *40*, 1811–1816. <https://doi.org/10.1002/grl.50424>
- Poloczanska, E. S., Brown, C. J., Sydeman, W. J., Kiessling, W., Schoeman, D. S., Moore, P. J., ... Duarte, C. M. (2013). Global imprint of climate change on marine life. *Nature Climate Change*, *3*, 919–925. <https://doi.org/10.1038/nclimate1958>
- Post, E., & Forchhammer, M. C. (2002). Synchronization of animal population dynamics by large-scale climate. *Nature*, *420*, 168–171. <https://doi.org/10.1038/nature01064>
- Pratt, J. D., & Mooney, K. A. (2013). Clinal adaptation and adaptive plasticity in *Artemisia californica*: Implications for the response of a foundation species to predicted climate change. *Global Change Biology*, *19*, 2454–2466. <https://doi.org/10.1111/gcb.12199>
- Reid, P. C., Hari, R. E., Beaugrand, G., Livingstone, D. M., Marty, C., Straile, D., ... Brown, R. (2016). Global impacts of the 1980s regime shift. *Global Change Biology*, *22*, 682–703. <https://doi.org/10.1111/gcb.13106>
- Schindler, D. E., Armstrong, J. B., & Reed, T. E. (2015). The portfolio concept in ecology and evolution. *Frontiers in Ecology and the Environment*, *13*, 257–263. <https://doi.org/10.1890/140275>
- Schindler, D. E., Hilborn, R., Chasco, B., Boatright, C. P., Quinn, T. P., Rogers, L. A., & Webster, M. S. (2010). Population diversity and the portfolio effect in an exploited species. *Nature*, *465*, 609–612. <https://doi.org/10.1038/nature09060>
- Schroder, I. D., Black, B. A., Sydeman, W. J., Bograd, S. J., Hazen, E. L., Santora, J. A., & Wells, B. K. (2013). The North Pacific High and wintertime pre-conditioning of California current productivity. *Geophysical Research Letters*, *40*, 1–6.
- Schwing, F. B., Murphree, T., & Green, P. M. (2002). The Northern Oscillation Index (NOI): A new climate index for the northeast Pacific. *Progress in Oceanography*, *53*, 115–139. [https://doi.org/10.1016/S0079-6611\(02\)00027-7](https://doi.org/10.1016/S0079-6611(02)00027-7)
- Schwing, F. B., O'farrell, M., Steger, J. M., & Baltz, K. (1996). Coastal upwelling indices, West Coast of North America, 1946–1995. NOAA Technical Memorandum NOAA-TM-NMFS-SWFC-231. National Oceanic and Atmospheric Administration, Washington, DC, 144 pp.
- Seager, R., Hoerling, M., Schubert, S., Wang, H., Lyon, B., Kumar, A., ... Henderson, N. (2015). Causes of the 2011–14 California Drought. *Journal of Climate*, *28*, 6997–7024. <https://doi.org/10.1175/JCLI-D-14-00860.1>
- Sheppard, L., Bell, J. R., Harrington, R., & Reuman, D. C. (2016). Changes in large-scale climate alter spatial synchrony of aphid pests. *Nature Climate Change*, *6*, 610–613. <https://doi.org/10.1038/nclimate2881>
- Shestakova, T. A., Gutiérrez, E., Kiryanov, A. V., Camarero, J. J., Génova, M., Knorre, A. A., ... Voltas, J. (2016). Forests synchronize their growth in contrasting Eurasian regions in response to climate warming. *Proceedings of the National Academy of Sciences of the United States of America*, *113*, 662–667. <https://doi.org/10.1073/pnas.1514717113>
- Slack, J. R., Jumb, A., & Landwehr, J. (1993). *Hydro-climatic data network (HCDN) Streamflow data set, 1874–1988*. Water-Resources Investigations Report 93-4076, Reston, VA.
- Stahle, D. W., Griffin, R. D., Meko, D. M., Therrell, M. D., Edmondson, J. R., Cleaveland, M. K., ... Dettinger, M. D. (2013). The ancient blue oak woodlands of California: Longevity and hydro-climatic history. *Earth Interactions*, *17*, 1–12. <https://doi.org/10.1175/2013EI000518.1>
- Sydeman, W. J., Santora, J. A., Thompson, S. A., Marinovic, B. M., & Di Lorenzo, E. (2013). Increasing variance in North Pacific climate relates to unprecedented pelagic ecosystem variability off California. *Global Change Biology*, *19*, 1662–1675. <https://doi.org/10.1111/gcb.12165>
- Thompson, R. M., Beardall, J., Beringer, J., Grace, M., & Sardina, P. (2013). Means and extremes: Building variability into community-level climate change experiments. *Ecology Letters*, *16*, 799–806. <https://doi.org/10.1111/ele.12095>
- Thompson, S. A., Sydeman, W. J., Santora, J. A., Black, B. A., Suryan, R. M., Calambokidis, J., ... Bograd, S. J. (2012). Linking predators to seasonality of upwelling: Using food web indicators and path analysis to infer trophic connections. *Progress in Oceanography*, *101*, 106–120. <https://doi.org/10.1016/j.pcean.2012.02.001>
- Trouet, V., Babst, F., & Meko, M. (2018). Recent enhanced high-summer North Atlantic Jet variability emerges from three-century context. *Nature Communications*, *9*, 180. <https://doi.org/10.1038/s41467-017-02699-3>
- Wang, S. Y., Hippias, L., Gillies, R. R., & Yoon, J. H. (2014). Probable causes of the abnormal ridge accompanying the 2013–2014 California drought: ENSO precursor and anthropogenic warming footprint. *Geophysical Research Letters*, *41*, 3220–3226. <https://doi.org/10.1002/2014GL059748>
- Wigley, T. M. L., Briffa, K. R., & Jones, P. D. (1984). On the average value of correlated time-series, with applications in dendroclimatology and hydrometeorology. *Journal of Climate and Applied Meteorology*, *23*, 201–213. [https://doi.org/10.1175/1520-0450\(1984\)023<201:OTAVOC>2.0.CO;2](https://doi.org/10.1175/1520-0450(1984)023<201:OTAVOC>2.0.CO;2)

- Williams, A. P., Seager, R., Abatzoglou, J. T., Cook, B. I., Smerdon, J. E., & Cook, E. R. (2015). Contribution of anthropogenic warming to California drought during 2012-2014. *Geophysical Research Letters*, 42, 6819–6828. <https://doi.org/10.1002/2015GL064924>
- Wilson, R., Cook, E., D'arrigo, R., Riedwyl, N., Evans, M. N., Tudhope, A., & Allan, R. (2010). Reconstructing ENSO: The influence of method, proxy data, climate forcing and teleconnections. *Journal of Quaternary Science*, 25, 62–78. <https://doi.org/10.1002/jqs.1297>
- Zhou, Z. Q., Xie, S. P., Zheng, X. T., Liu, Q. Y., & Wang, H. (2014). Global warming-induced changes in El Niño teleconnections over the North Pacific and North America. *Journal of Climate*, 27, 9050–9064. <https://doi.org/10.1175/JCLI-D-14-00254.1>

## SUPPORTING INFORMATION

Additional Supporting Information may be found online in the supporting information tab for this article.

**How to cite this article:** Black BA, van der Sleen P, Di Lorenzo E, et al. Rising synchrony controls western North American ecosystems. *Glob Change Biol*. 2018;24:2305–2314. <https://doi.org/10.1111/gcb.14128>